

Sliding Mode Control of Pitch-Rate of an F-16 Aircraft [★]

Ekprasit Promtun ^{*} Sridhar Seshagiri ^{**}

^{*} Aircraft Research and Development Office, Royal Thai Air Force,
Don Muang, Bangkok, Thailand (promtun@rohan.sdsu.edu)

^{**} Department of Electrical and Computer Engg., San Diego State
University, USA (seshagir@kahuna.sdsu.edu)

Abstract: The control of the longitudinal flight dynamics of an F-16 aircraft is challenging because the system is highly nonlinear, and also non-affine in the input. We consider a sliding mode control design based on linearization of the aircraft, with the altitude h and velocity V (Mach number) as the trim variables. The design further exploits the modal decomposition of the dynamics into its short-period and phugoid approximations. The primary design objective is model-following of the pitch rate q , which is the preferred system for aircraft approach and landing. Regulation of the aircraft velocity V (or the Mach-hold autopilot) is also considered, but as a secondary objective. It is shown that the inherent robustness of the SMC design provides a convenient way to design controllers without gain scheduling, with a steady-state response that is comparable to that of a conventional gain-scheduled approach with integral control, but with improved transient performance. Finally, we apply the recently developed technique of “conditional integrators” to achieve asymptotic regulation with constant exogenous signals, without degrading the transient response. Through extensive simulation on the nonlinear multiple-input multiple-output (MIMO) longitudinal model of the F-16 aircraft, we show that the conditional integrator design outperforms the one based on the conventional approach, without requiring any scheduling.

Keywords: F-16 Longitudinal Dynamics; Pitch-Rate Control; Sliding-mode Control; Integral Control; Model Following.

1. INTRODUCTION

The dynamic response characteristics of aircraft are highly nonlinear. Traditionally, flight control systems have been designed using mathematical models of the aircraft linearized at various flight conditions, with the controller parameters or gains “scheduled” or varied with the flight operating conditions. Various robust multivariable techniques including linear quadratic optimal control (LQR/LQG), H_∞ control, and structured singular value μ -synthesis have been employed in controller design, an excellent and exhaustive compendium of which is available in Magni et al. [1998]. Nonlinear design techniques such as dynamic inversion have been used in Adams et al. [1994], Reigelsperger and Banda [1998], Snell et al. [1992], while a technique that combines model inversion control with an online adaptive neural network to “robustify” the design is described in Rysdyk and Calise [2005], and a nonlinear adaptive design based on backstepping and neural networks in Lee and Kim [2001]. A succinct “industry perspective” on flight control design, including the techniques of robust control (H_∞ , μ -synthesis), LPV control, dynamic inversion, adaptive control, neural networks, and more, can be found in Balas [2003].

Our interest is in the design of robust sliding mode control (SMC) for the longitudinal flight dynamics of a F-16 aircraft, and is based on a recent technique in Seshagiri and Khalil [2005] for introducing integral action in sliding mode control. Our primary emphasis is on the transient and steady-state performance of control of the aircraft’s pitch rate, with the steady-state performance and disturbance rejection of the aircraft’s velocity as a (minor) secondary objective. Our design exploits the modal decomposition of the linearized dynamics into its short-period and phugoid approximations, and our controller has a very simple structure. It is simply a high-gain PI controller with an “anti-windup” integrator, followed by saturation. This controller structure is a special case of a general design for robust output regulation for multiple-input multiple-output (MIMO) nonlinear systems transformable to the normal form, with analytical results for stability and performance described in Seshagiri and Khalil [2005]. Through extensive simulations, we show that this design outperforms a traditional gain-scheduled controller design based on the polynomial approach to model-following design.

The rest of this paper is organized as follows. In Section 2, we describe the nonlinear mathematical aircraft model, its linearization and the decomposition of the dynamics into the short-period and phugoid modes. The design of the pitch controller is taken up in Section 3, and

[★] The first author was financially supported in part by the Royal Thai Air Force.

simulation results showing the efficacy of the design, along with comparisons to gain scheduled controllers using the (linear) transfer-function based polynomial approach to model-following are presented in Section 4. Finally, a summary of our work and some suggestions for possible extensions are provided in Section 5.

2. 3-DOF LONGITUDINAL MODEL

The decoupled equations of pure longitudinal motion (assuming no thrust-vectoring) of a six degree-of-freedom (DOF) aircraft can be described by the 5th order nonlinear state model

$$\left. \begin{aligned} \dot{V} &= \frac{\bar{q}S\bar{c}q}{2mV} [C_{xq}(\alpha) \cos \alpha + C_{zq}(\alpha) \sin \alpha] - g \sin(\theta - \alpha) \\ &+ \frac{\bar{q}S}{m} [C_x(\alpha, \delta_e) \cos \alpha + C_z(\alpha, \delta_e) \sin \alpha] + \frac{T}{m} \cos(\alpha) \\ \dot{\alpha} &= q \left[1 + \frac{\bar{q}S\bar{c}}{2mV^2} (C_{zq}(\alpha) \cos \alpha - C_{xq} \sin \alpha) \right] \\ &+ \frac{\bar{q}S}{mV} [C_z(\alpha, \delta_e) \cos \alpha - C_x(\alpha, \delta_e) \sin \alpha] \\ &+ \frac{g}{V} \cos(\theta - \alpha) - \frac{T}{mV} \sin(\alpha) \\ \dot{\theta} &= q \\ \dot{q} &= \frac{\bar{q}S\bar{c}q}{2I_y V} [\bar{c}C_{mq}(\alpha) + \Delta C_{zq}(\alpha)] \\ &+ \frac{\bar{q}S\bar{c}}{I_y} \left[C_m(\alpha, \delta_e) + \frac{\Delta}{\bar{c}} C_z(\alpha, \delta_e) \right] \\ \dot{h} &= V \sin(\theta - \alpha) \end{aligned} \right\} \quad (1)$$

where V , α , θ , q and h are the aircraft's velocity, angle-of-attack, pitch attitude, pitch rate and altitude respectively, T the thrust force, δ_e the elevator angle, m the mass of the aircraft, I_y the moment of inertia about the Y-body axis, $\bar{q} = \bar{q}(h, V) = \frac{1}{2}\rho(h)V^2$ the dynamic pressure, S the wing area, Δ the distance between the reference and actual center of gravity, $C_m(\cdot)$ the pitching moment coefficient along the Y-body axis, $C_{mq}(\cdot) = \frac{\partial C_m}{\partial q}$ the variation of C_m with pitch rate, $C_x(\cdot)$ and $C_z(\cdot)$ the force coefficients along the stability X and Z axes respectively, and $C_{xq}(\cdot)$ and $C_{zq}(\cdot)$ the variations of these coefficients with the pitch rate. The system (1) can be compactly written in standard form as

$$\dot{x} = f(x, u), \quad y = h(x, u) \quad (2)$$

where

$$x = [V \ \alpha \ \theta \ q \ h]^T \in R^5$$

is the state vector, and

$$u = [T \ \delta_e]^T \in R^2, \quad y = [V \ h]^T \in R^2$$

are the control input and the measured output respectively¹. For the purpose of simulating our controller design, we build a Simulink model for the longitudinal dynamics of a scaled F-16 aircraft model based on NASA Langley wind tunnel tests, as described in Russell [2003], Stevens and Lewis [2003], and based on the work in Nguyen et al. [1979]. In particular, the model that we build corresponds to the *low fidelity* F-16 longitudinal model in Russell [2003], and to the longitudinal F-16 model developed in Lu [2004], but without thrust vectoring. For

¹ We use y for the purpose of linearization, but the "regulated outputs" are the pitch-rate q and the velocity V .

the aerodynamic data we use the approximate data in Nguyen et al. [1979], Stevens and Lewis [2003], with the mass and geometric properties as listed in Table 1. The

Table 1. Mass and geometric properties.

Parameter	Symbol	Value
Weight	W (lb)	20500
Moment of inertia	I_y (slug-ft ²)	55814
Wing area	S (ft ²)	300
Mean aerodynamic chord	\bar{c} (ft)	11.32
Reference CG location	$x_{cg,ref}$	$0.35\bar{c}$

coefficients $C_{xq}(\alpha)$, $C_{zq}(\alpha)$, $C_{mq}(\alpha)$, $C_x(\alpha, \delta_e)$, $C_z(\alpha, \delta_e)$, and $C_m(\alpha, \delta_e)$ are taken from Nguyen et al. [1979], Stevens and Lewis [2003], and are included in [Promtun, 2007, Appendix A.1] in tabular form. In the simulation, the data is interpolated linearly between the points, and extrapolated beyond the table boundaries.

It can easily be verified that given any desired equilibrium value $\hat{y} = [\hat{V}, \hat{h}]^T$, there exist a unique equilibrium input $u = \hat{u}$ and state $x = \hat{x}$, such that $f(\hat{x}, \hat{u}) = 0$. Defining the perturbation input, state, and output respectively by

$$u_\delta = u - \hat{u}, \quad x_\delta = x - \hat{x}, \quad y_\delta = y - \hat{y} \quad (3)$$

results in the linear approximation

$$\dot{x}_\delta = Ax_\delta + Bu_\delta, \quad y_\delta = Cx_\delta + Du_\delta \quad (4)$$

where

$$A = \frac{\partial f}{\partial x}(\hat{x}, \hat{u}), \quad B = \frac{\partial f}{\partial u}(\hat{x}, \hat{u}), \quad C = \frac{\partial h}{\partial x}(\hat{x}, \hat{u}), \quad D = \frac{\partial h}{\partial u}(\hat{x}, \hat{u}) \quad (5)$$

Since the drag coefficients $C_i(\cdot)$ are not specified explicitly as functions of their arguments, but in tabular form (as look-up data), we use numerical techniques to solve for the trim (equilibrium) points and to compute the linearization. The *flight envelope* that we use for computing the trim conditions and the linearization is the cross product set $(\hat{V}, \hat{h}) \in \Omega_V \times \Omega_h$, where $\Omega_V = [300, 900]$ ft/s in steps of 100, while $\Omega_h = [5000, 40000]$ ft in steps of 5000. In order to simplify subsequent notation, we reorder the state variables as follows. Define

$$z = [\alpha \ q \ V \ \theta \ h]^T \stackrel{\text{def}}{=} Ex \quad (6)$$

and define $z_\delta = z - \hat{z}$, so that

$$\dot{z}_\delta = EAE^{-1}z_\delta + EBu_\delta \stackrel{\text{def}}{=} A_z z_\delta + B_z u_\delta \quad (7)$$

Partitioning the states as

$$z^T = [z_1^T \ z_2^T \ h], \quad z_1 \stackrel{\text{def}}{=} [\alpha \ q]^T, \quad z_2 \stackrel{\text{def}}{=} [V \ \theta]^T$$

it follows that we can rewrite (7) as

$$\begin{bmatrix} \dot{z}_{1\delta} \\ \dot{z}_{2\delta} \\ \dot{h}_\delta \end{bmatrix} = \begin{bmatrix} A_{11} & A_{12} & A_{13} \\ A_{21} & A_{22} & A_{23} \\ * & * & 0 \end{bmatrix} \begin{bmatrix} z_{1\delta} \\ z_{2\delta} \\ h_\delta \end{bmatrix} + \begin{bmatrix} B_{11} & B_{12} \\ B_{21} & B_{22} \\ 0 & 0 \end{bmatrix} \begin{bmatrix} T_\delta \\ \delta_{e\delta} \end{bmatrix} \quad (8)$$

Assumption 1. For each linearization

$$A_{12} \approx A_{13} \approx A_{23} \approx B_{11} \approx 0$$

While this has been verified numerically in this work, for each operating condition, an analytical discussion can be found in [Stevens and Lewis, 2003, Chapter 4]. It follows from Assumption (1) that the MIMO linearization (7) can be further decoupled into the SISO-like state equations

$$\begin{aligned} \dot{z}_{1\delta} &= \begin{bmatrix} \dot{\alpha}_\delta \\ \dot{q}_\delta \end{bmatrix} \approx A_{11} \begin{bmatrix} \alpha_\delta \\ q_\delta \end{bmatrix} + B_{12} \delta_{e_\delta} \\ \dot{z}_{2\delta} &= \begin{bmatrix} \dot{V}_\delta \\ \dot{\theta}_\delta \end{bmatrix} \approx A_{21} \begin{bmatrix} \alpha_\delta \\ q_\delta \end{bmatrix} + A_{22} \begin{bmatrix} V_\delta \\ \theta_\delta \end{bmatrix} + B_{21} T_\delta + B_{22} \delta_{e_\delta} \end{aligned} \quad (9)$$

By way of physical insight into this decoupling, we mention that it is well known that aircraft dynamics behave differently to elevator and throttle inputs. In particular, the former excites a “natural mode” where α and θ vary together, causing very little change in the flight-path angle $\gamma \stackrel{\text{def}}{=} \theta - \alpha$, and is called the *short period* mode. The *phugoid* mode is excited by the thrust input, which has very little effect on the short-period mode. It is clear from (9) then that the dynamics of the variables z_1 and z_2 constitute the short-period and phugoid modes respectively.

We exploit the decoupling in (9) in our controller designs in the next section. In particular, we use the elevator δ_e to control the pitch rate q , and the thrust T to control the aircraft’s velocity V . This makes the control design problem much simpler than the one for the original MIMO system. Note that we did not include the altitude equation in (9). This is because (i) h is not a regulated output (we mentioned earlier that we wish to regulate q and V) and (ii) since $A_{13} \approx A_{23} \approx 0$, h does not enter the short-period and phugoid approximations explicitly, and is therefore not important for the control design. However, it does appear implicitly in the computation of the coefficient matrices. In the next section, we take up the controller design starting from the fourth-order system (9), which is obtained for each trim condition $[\hat{V}, \hat{h}]^T$. However, the design is evaluated on the full fifth order nonlinear state model (2).

3. CONTROL DESIGN

Our primary control objective in this work is the design of a pitch-rate command system. It is well-known that a deadbeat response to pitch-rate commands is well suited to precise tracking of a target by means of a sighting device, and that control of the pitch rate is also the preferred system for approach and landing. Since the original system is MIMO, we also consider, but as a secondary objective, a Mach-hold autopilot, which is chiefly used on military aircraft during climb and descent. During a climb the throttles may be set at a fairly high power level, and feedback of Mach number to the elevator is used to achieve a constant-Mach climb. The speed will vary over the range of altitude, but the constant Mach number provides the best fuel efficiency. Similarly, a descent will be flown at constant Mach with the throttles near idle.

For the pitch-rate command system, the entire dynamic response is important, and we assume that the desired specifications are encapsulated in a reference model. We employ the same reference model as in Barbu et al. [2005], Hess and Kalteis [1991]

$$G_m(s) = \frac{q_m(s)}{q_d(s)} = \frac{1.4s + 1}{s^2 + 1.5s + 1}$$

where q_d is the pitch rate pilot command. Our approach to control design for the pitch-rate is based on minimum-phase systems transformable to the normal form

$$\begin{aligned} \dot{\eta} &= \phi(\eta, \xi) \\ \dot{\xi} &= A_c \xi + B_c \gamma(x) [u - \alpha(x)] \\ y &= C_c \xi \end{aligned}$$

where $x \in R^n$ is the state, u the input, ρ is the system’s relative degree, $\xi \in R^\rho$ the output and its derivatives up to order $\rho - 1$, $\eta \in R^{n-\rho}$ the part of the state corresponding to the internal dynamics, and the triple (A_c, B_c, C_c) a canonical form representation of a chain of ρ integrators. A SMC design for such a system (or actually a more general MIMO system) was carried out in Seshagiri and Khalil [2005], with the assumption that the internal dynamics $\dot{\eta} = \phi(\eta, \xi)$ are input-to-state stable (ISS) with ξ as the driving input. We apply this design to the short period approximation (9), with δ_{e_δ} as input and q_δ as output. Note that this is a relative degree $\rho = 1$ system. In order to apply the technique in Seshagiri and Khalil [2005], we need to transform the system to normal form and check internal stability. The next proposition states these properties, and is straightforward to verify.

Proposition 1. Consider the short-period approximation

$$\begin{bmatrix} \dot{\alpha}_\delta \\ \dot{q}_\delta \end{bmatrix} \stackrel{\text{def}}{=} \begin{bmatrix} a_{\alpha\alpha} & a_{\alpha q} \\ a_{q\alpha} & a_{qq} \end{bmatrix} \begin{bmatrix} \alpha_\delta \\ q_\delta \end{bmatrix} + \begin{bmatrix} b_{\alpha\delta} \\ b_{q\delta} \end{bmatrix} \delta_{e_\delta}$$

with output q_δ . Then (i) $b_{q\delta} > 0$, (ii) the (invertible) change of coordinates

$$\begin{bmatrix} \xi \\ \eta \end{bmatrix} \stackrel{\text{def}}{=} \begin{bmatrix} 0 & 1 \\ 1 & -\frac{b_{\alpha\delta}}{b_{q\delta}} \end{bmatrix} \begin{bmatrix} \alpha_\delta \\ q_\delta \end{bmatrix}$$

transforms the system to normal form

$$\begin{bmatrix} \dot{\eta} \\ \dot{\xi} \end{bmatrix} \stackrel{\text{def}}{=} \begin{bmatrix} a_{\eta\eta} & a_{\eta\xi} \\ a_{\xi\eta} & a_{\xi\xi} \end{bmatrix} \begin{bmatrix} \eta \\ \xi \end{bmatrix} + \begin{bmatrix} 0 \\ 1 \end{bmatrix} \delta_{e_\delta}$$

$$q_\delta = \xi$$

and (iii) $a_{\eta\eta} < 0$, i.e., the system is minimum-phase.

As in the previous section, we have only verified parts (i) and (iii) of Proposition 1 numerically, for each trim condition, but an analytic discussion based on the stability derivatives can be found in Stevens and Lewis [2003].

Proposition 1 allows us to SMC controller design in Seshagiri and Khalil [2005] for the q -dynamics. For completeness, we briefly point out the ingredients of such a design. In the absence of integral control, a standard SMC design for such a system takes the form $u = -k \text{sgn}(e)$, where $e = q - q_m$ is the tracking error ², and $\text{sgn}(s)$ the signum function. It is easy to show that the design achieves asymptotic error regulation for “sufficiently large” k . In order to alleviate the chattering problem (see Young et al. [1999]) that is common with ideal discontinuous control, it is common to replace the above design with its continuous approximation $u = -k \text{sat}\left(\frac{e}{\mu}\right)$, where $\text{sat}(s)$ is the standard saturation function, and μ the width of the “boundary layer”. This modification can reduce chattering, but at the expense of only achieving practical regulation of the error e , with $|e| = O(\mu)$. Consequently, reducing the steady-state error requires making μ small, which again leads to chattering. In order to achieve asymptotic error regulation with continuous SMC, robustly in the presence

² Note that for each trim condition $\hat{q} = 0$, so that $q_\delta \equiv q$, which is why we simply use q in defining e .

of disturbances and unknown parameter values, one can augment the system with an integrator driven by the error, i.e. $\dot{\sigma} = e$, and include the integrator output σ as part of the sliding variable s . Such a design can be found in Khalil [2000], where it is shown that the design reduces to a PI controller, followed by saturation. The drawback of this design is that the recovery of the steady-state asymptotic error regulation (of ideal SMC) is achieved at the expense of transient performance degradation, in part due to an increase in system order, and in part as a consequence of controller saturation interacting with the integrator, resulting in “integrator windup”.

The “conditional integrator” design in Seshagiri and Khalil [2005] is a novel way to introduce integral action in continuous SMC, while retaining the transient response of ideal SMC (without integral control). In this approach, we modify the sliding surface design to

$$s = k_0\sigma + e \quad (10)$$

where $k_0 > 0$ is arbitrary, and σ is the output of

$$\dot{\sigma} = -k_0\sigma + \mu \text{sat}(s/\mu), \quad \sigma(0) = 0 \quad (11)$$

To see the relation of (11) to integral control, observe that inside the boundary layer $\{|s| \leq \mu\}$, (11) reduces to $\dot{\sigma} = e$, which implies that $e = 0$ at equilibrium. Thus (11) represents a “conditional integrator” that provides integral action only inside the boundary layer. The control is simply taken as the continuous approximation of ideal SMC, i.e.,

$$\delta_e = -k \text{sat}(s/\mu) = -k \text{sat}\left(\frac{k_0\sigma + e}{\mu}\right) \quad (12)$$

This completes the design of the pitch-rate controller, and analytical results for stability and performance of such a design applied to control-affine minimum-phase MIMO nonlinear systems can be found in Seshagiri and Khalil [2005]. Note that we have simply applied the technique in Seshagiri and Khalil [2005] to the linear short period approximation (9).

Since we are only interested in the Mach-hold autopilot (for V) as a secondary objective (of minor importance), and this is usually designed simply to meet specifications on steady-state error and disturbance rejection, we only design a simple PI controller for the thrust T to regulate V . To do so, we start with the observation that from $\dot{\theta} = q$, the matrices of the linearization in (8) are of the form

$$A_{21} = \begin{bmatrix} * & * \\ 0 & 1 \end{bmatrix}, A_{22} = \begin{bmatrix} * & * \\ 0 & 0 \end{bmatrix}, B_{21} = \begin{bmatrix} * & * \\ 0 & 0 \end{bmatrix}, B_{22} = \begin{bmatrix} * & * \\ 0 & 0 \end{bmatrix}$$

so that we the equations for the $z_{2\delta}$ -subsystem in (9) can be further simplified as

$$\begin{aligned} \dot{V}_\delta &\stackrel{\text{def}}{=} a_{V\alpha}\alpha_\delta + a_{Vq}q_\delta + a_{VV}V_\delta + a_{V\theta}\theta_\delta + b_{VT}T_\delta + b_{V\delta}\delta_{e\delta} \\ \dot{\theta}_\delta &= q_\delta \end{aligned} \quad (13)$$

It can be verified that for each trim condition, $a_{VV} < 0$, i.e., the V_δ -subsystem is Hurwitz, and it is clear (looking at the \dot{V} equation) that $b_{VT} = g/m$. We view the term $a_{V\alpha}\alpha_\delta + a_{Vq}q_\delta + a_{V\theta}\theta_\delta + b_{V\delta}\delta_{e\delta}$ as constituting a “matched disturbance”, and simply design T_δ as the PI controller

$$T_\delta = -k_P V_\delta - k_I \sigma_V, \quad \dot{\sigma}_V = V_\delta \quad (14)$$

with the gains $k_p, k_I > 0$ chosen to assign the eigenvalues of the 2nd-order system with states σ_V and V_δ at desired pole locations. This completes the design of the Mach-hold autopilot controller.

We do not provide a rigorous analysis since our design is based on linearization of a non-affine in the input system, and the analytical results of Seshagiri and Khalil [2005] do not directly apply to this design. However, we believe that our controller achieves boundedness of all states, and asymptotic error regulation of the error e , which can be explained as follows. The SMC (12) achieves robust regulation of the pitch-rate q , provided the value of k is “sufficiently large”. The variable α is bounded since the system is minimum-phase. The variable θ evolves according to $\dot{\theta} = q$, and hence is bounded whenever q is. The PI controller (14) achieves boundedness of the velocity V . Finally, from the equation of \dot{h} , it follows that h is bounded for all finite time whenever V is, so that with our SMC and PI controllers for δ_e and T respectively, all the states of the closed-loop system are bounded.

4. SIMULATION RESULTS

Numerical values of the SMC parameters that we use in all the simulations are $k_0 = 10$, and that $k = 25$, so that $-25 \leq \delta_e \leq 25$, which are the limits mentioned in Russell [2003], Sonneveldt [2006]. The boundary layer width μ is chosen “sufficiently small”, and we will say more on this when we present the simulation results. The control is always tested on the full 5th order nonlinear model. For comparison, we also plot the results from a classical gain-scheduled approach to model following, with the details of the design described in [Promtun, 2007, Chapter 3]. The initial values in all simulations correspond to trim conditions with $(\hat{V}, \hat{h}) = (600 \text{ ft/s}, 20000 \text{ ft})$.

Our first simulation shows the performance of a continuous SMC with no integral action, i.e., $u = -k \text{sat}\left(\frac{e_1}{\mu}\right)$ when the pilot pitch-rate command q_d is a doublet, for 2 different values of magnitude of q_d , 5 deg/s and 30 deg/s. The results are shown in Figure 1, plotted for 2 different values of μ in the SMC design, and we see that the performance of the SMC is superior to the gain-scheduled approach. We have had to clip the y-axis limits in the error subplots so that the difference between the errors for $\mu = 0.1$ and $\mu = 0.01$ can be observed. For the first error subplot, corresponding to $q_d = 5$, the error for the polynomial approach is roughly between $\approx \pm 1$, while we have limited the plot axis to ± 0.1 . Similarly, for the error subplot corresponding to $q_d = 30$, the error for the polynomial approach is roughly between $\approx \pm 7$, while we have limited the plot axis to ± 0.7 . By contrast, the error for the SMC with $\mu = 0.1$ is roughly less than 0.02 for $q_d = 5$, and less than 0.1 for $q_d = 30$ in “steady-state”. By steady-state, we refer to the period $t > 2s$. The reason for the relatively large peak error of about 0.5 (which itself is roughly 14 times smaller than the error with the polynomial approach !) is that the control reaches its saturation limits (in particular, $\delta = -25^\circ$ between 0.7 and 1.35s) with the SMC approach. We do not apply saturation limits for the polynomial approach. In other words, this simulation shows that SMC with no gain-scheduling, no integral

control, and control saturation, outperforms the gain-scheduled polynomial approach controller with integral control and without saturation.

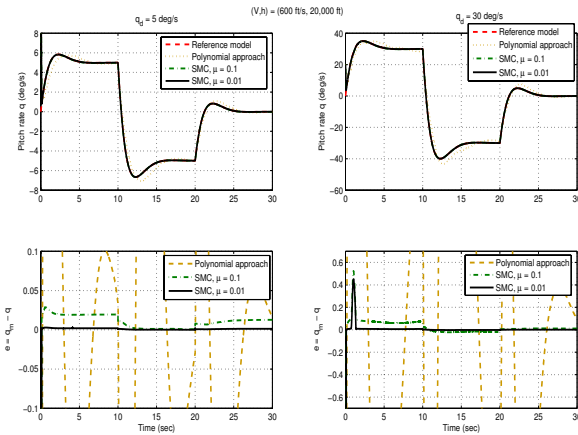


Fig. 1. Tracking errors with SMC: Nonlinear model, $q_d = 5$, and $q_d = 30$ deg/s.

In order to demonstrate the performance of the robustness of the SMC approach to matched disturbances, we assume that there is an input additive disturbance at the elevator input (which can alternately be thought of as offset of the trim value of δ_e), i.e., $\delta_e = \hat{\delta}_e + d$. Note that this disturbance effectively replaces δ_e in every equation in (1) by $\delta_e + d$. Figure 2 shows the simulation results for $d = 5$, and it is again clear that the SMC far outperforms the polynomial approach based controller design, with no gain scheduling requirements.

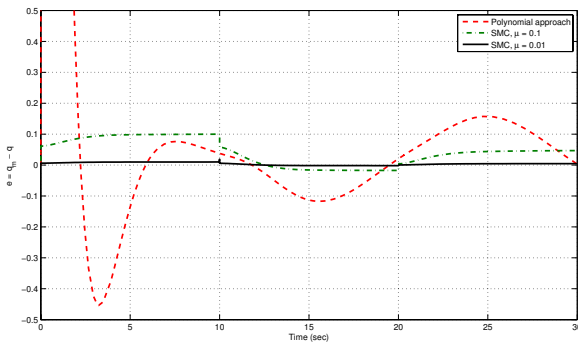


Fig. 2. Tracking errors with SMC: Full linear model with input additive disturbance.

Next, we repeat the first simulation, but with the conditional integrator. Since we have already plotted the results of SMC without integral control and shown that they are superior to the polynomial approach, we simply compare the errors for the SMC with and without integral control, and only do so for $q_d = 30$ deg/s. The simulation results are done for $\mu = 1$ and $\mu = 0.1$. The reason to include a larger value of μ is twofold (i) to demonstrate the fact that the inclusion of integral action means that we don't need to make μ very small to achieve regulation, only small enough to stabilize the equilibrium point, and (ii) to highlight the issue of chattering with small μ , which we relegate to the next simulation. The simulation results are

shown in Figure 3, from which two inferences might be drawn. The first is that, in the absence of integral control, since $|e| = O(\mu)$, we must decrease μ in order to achieve smaller steady-state errors, and this is clear from the two subplots. The second inference is that the inclusion of integral action decreases the steady-state error, and in fact, achieves asymptotic error regulation.

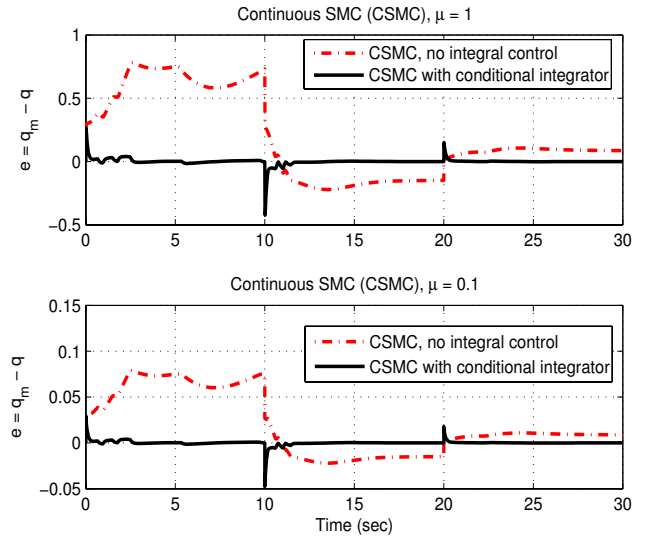


Fig. 3. Tracking errors with with conditional integrator SMC: Nonlinear model, $q_d = 30$ deg/s.

Next, we show decreasing μ , while reducing the steady-state error in an ideal scenario, can lead to chattering when there are switching imperfections such as delays. To demonstrate this, we repeat the previous simulation with a delay of 5ms (which is not really very large) preceding the input. The simulation results are shown in Figure 4, and we see **considerable chattering** in the control for $\mu = 0.1$, and we see that the control frequently hits the saturation lower limit. This chattering can excite unmodeled high-frequency dynamics, degrade system performance, cause actuator wear, and even result in instability. In order that chattering be avoided, we must make μ large, but doing so without integral control will lead to larger errors, since $|e| = O(\mu)$. The inclusion of integral control using conditional integrators offers a way to retain transient performance of ideal SMC and achieve zero steady-state error, without having to make μ very small, so that chattering can be avoided, and this is readily inferred from Figure 4.

Lastly, before we summarize our results, we present our results for velocity tracking with the PI controller, with gains $k_P = 828.4$ and $k_I = 191.2$ chosen to assign the roots of the closed-loop characteristic polynomial

$$\lambda^2 + b_{VT}k_P\lambda + b_{VT}k_I$$

at -0.3 and -1. The desired velocity reference is the output of the first order filter $H(s) = \frac{1}{s+1}$, to which the input is a doublet-like signal with an initial value of 600 ft/s, changing to 500 ft/s at $t = 17s$, and to 700 ft/s at $t = 35s$. The results are shown in Figure 5, and it is clear that this simple controller achieve robust regulation, even though its transient performance is not very good, as expected. We can improve the design of the velocity controller using

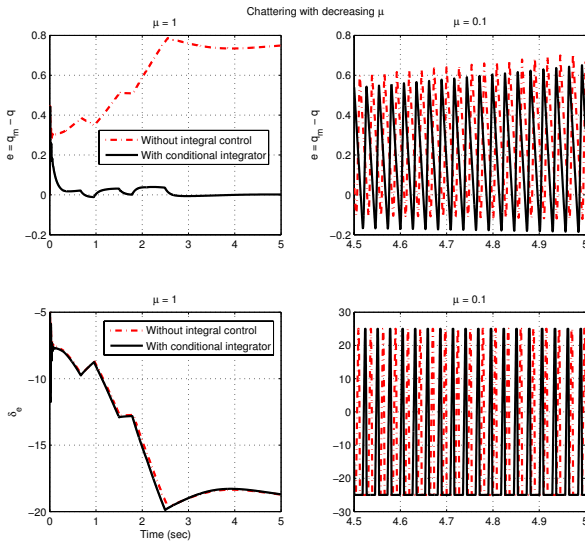


Fig. 4. Time-delays and chattering in continuous SMC.

techniques like SMC or other robust linear techniques, but do not pursue it, since velocity control is only a secondary objective.

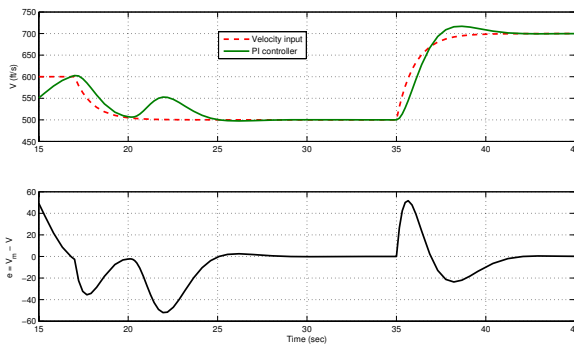


Fig. 5. Velocity (Mach-hold) autopilot response to velocity command: PI controller.

5. CONCLUSIONS

We have presented a new SMC design for control of the pitch-rate of an F-16 aircraft, based on the conditional integrator design of Seshagiri and Khalil [2005]. The design exploits the short-period approximation of the linearized flight dynamics. The robustness of the method to modeling uncertainty, disturbances, and time-delays was demonstrated through extensive simulation, and the simulation results showed that the method outperforms, without any scheduling, the transient and steady-state performance of a conventional gain-scheduled model-following controller. The conditional integrator design allows us to introduce integral action to achieve zero steady-state errors without degrading the transient performance of ideal SMC. While we did not present any analytical results, we believe, that analytical results based on a control-affine approximation of the nonlinear system should be possible. Consequently, we believe that the results presented in this paper are a promising start to demonstrate the efficacy of the conditional integrator based SMC design to flight control.

REFERENCES

- R.J. Adams, J.M. Buffington, and S.S. Banda. Design of nonlinear control laws for high-angle-of-attack flight. *Jnl. Guidance, Control, and Dynamics*, 17(4):737–745, 1994.
- G.J. Balas. Flight control law design: An industry perspective. *European Jnl. of Ctrl.*, 9(2-3):207–226, 2003.
- C. Barbu, S. Galeani, A.R. Teel, and L. Zaccarian. Non-linear anti-windup for manual flight control. *Intl. Jnl. of Ctrl.*, 78(14):1111–1129, 2005.
- R.A. Hess and R.M. Kalteis. Technique for predicting longitudinal pilot-induced oscillations. *Jnl. Guidance, Control, and Dynamics*, 14:198–204, 1991.
- H.K. Khalil. Universal integral controllers for minimum phase nonlinear systems. *IEEE Trans. Aut. Ctrl.*, 45(3):490–494, 2000.
- T. Lee and Y. Kim. Nonlinear adaptive flight control using backstepping and neural networks controller. *Jnl. Guidance, Control, and Dynamics*, 24(4):675–682, 2001.
- B. Lu. *Linear Parameter-Varying Control of an F-16 Aircraft at High Angle of Attack*. PhD thesis, North Carolina State University, 2004.
- J-F. Magni, S. Bennani, and J. Terlouw (Eds). *Robust Flight Control: A Design Challenge*. Lecture Notes in Control and Information Sciences - Vol 224. Springer, 1998.
- L.T. Nguyen, M.E. Ogburn, W.P. Gillert, K.S. Kibler, P.W. Brown, and P.L. Deal. Simulator study of stall/post-stall characteristics of a fighter airplane with relaxed longitudinal static stability. *NASA Technical Paper 1538*, 1979.
- E. Promptun. *Sliding Mode Control of F-16 Longitudinal Dynamics*. MS. Thesis, San Diego State University, San Diego, USA, 2007.
- W.C. Reigelsperger and S.S. Banda. Nonlinear simulation of a modified F-16 with full-envelope control laws. *Control Engineering Practice*, 6:309–320, 1998.
- Richard S. Russell. Non-linear F-16 simulation using Simulink and Matlab. Technical report, University of Minnesota, June 2003.
- R. Rysdyk and A.J. Calise. Robust nonlinear adaptive flight control for consistent handling qualities. *IEEE Trans. Aut. Ctrl.*, 13(6):896–910, 2005.
- S. Seshagiri and H.K. Khalil. Robust output feedback regulation of minimum-phase nonlinear systems using conditional integrators. *Automatica*, 41(1):43–54, 2005.
- S.A. Snell, D.F. Enns, and Jr. W.L. Garrard. Nonlinear inversion flight control for a supermaneuverable aircraft. *Jnl. Guidance, Control, and Dynamics*, 15(4):976–984, 1992.
- Lars Sonneveldt. Nonlinear F-16 model description. Technical report, Delft University of Technology, The Netherlands, June 2006.
- B.L. Stevens and F.L. Lewis. *Aircraft Control and Simulation*. John Wiley & Sons, Inc., 2 edition, 2003.
- K.D. Young, V.I. Utkin, and U. Ozguner. A control engineer's guide to sliding mode control. *IEEE Trans. Ctrl. Sys. Tech.*, 7(3):328–342, 1999.